LAWRENCE
LIVERMORE
NATIONAL
LABORATORY

LLNL-CONF-412042

# Finite Element Modeling of the Deformation of a Thin Magnetoelastic Film Compared to a Membrane Model

M. Barham, D. White, D. Steigmann, R. Rudd

April 9, 2009

2009 IEEE International Magnetics Conference
Sacramento, CA, United States
May 4, 2009 through May 8, 2009

## Disclaimer

# Finite Element Modeling of the Deformation of a Thin Magnetoelastic Film Compared to a Membrane Model

M. Barham[1,2], D. White[2], D. J. Steigmann[1] and R. E. Rudd[2]

[1] Mechanical Engineering, University of California Berkeley, Berkeley, CA 94720, USA
[2] Lawrence Livermore National Laboratory, Livermore, CA 94550, USA

**Recently a new class of biocompatible elastic polymers loaded with small ferrous particles (magnetoelastomer) was developed at Lawrence Livermore National Laboratory. This new material was formed as a thin film using spin casting. The deformation of this material using a magnetic field has many possible applications to microfluidics. Two methods will be used to calculate the deformation of a circular magneto-elastomeric film subjected to a magnetic field. The first method is an arbitrary Lagrangian-Eulerian (ALE) finite element method (FEM) and the second is based on nonlinear continuum electromagnetism and continuum elasticity in the membrane limit. The comparison of these two methods is used to test/validate the finite element method.**

*Index Terms*— **Magnetoelasticity, Finite element methods, Magnetic Membrane, Microfluidics**

## I. Introduction

Recently a new class of biocompatible elastic polymers loaded with small ferrous particles (magnetoelastomer) has been developed at Lawrence Livermore National Laboratory. The magnetoelastic material consists of a mixture of polydimethylsiloxane (PDMS), iron powder and surfactants. The surfactant was used to increase dispersion of the iron particles. Thorough mixing was used to optimize the dispersion of the iron into the PDMS matrix and to break up large iron agglomerates. The material is formed into a thin film using spin casting, see Fig. 1 for a photo and a close up.

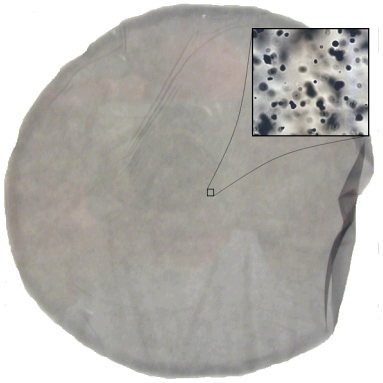

Fig. 1. Photo of magnetoelastic film and magnification

An applied magnetic field will deform the film. The deformation of this film from the applied magnetic field has many possible applications, particularly in microfluidic pumps and pressure regulators. Two methods will be used to calculate the equilibrium deformation of a circular magnetoelastomeric film subjected to a magnetic field. The first method is a computational approach employing the arbitrary Lagrangian-Eulerian (ALE) finite element method (FEM) for the full 3D finite thickness equations; this approach will be discussed in Section II. The second method is an analytical approach employing a membrane approximation; it is discussed in Section III. Results for both methods are presented in Section IV and a comparison of the two methods and a conclusion are presented in Section V.

Digital Object Identifier inserted by IEEE

## II. Finite Element Model

The finite element method is based on a coupling of the full three-dimensional equations of dynamic elasticity coupled with low-frequency (eddy current approximation) electromagnetics. The elastic equations are solved using the standard Galerkin method with linear nodal basis functions and implicit Hilber-Hughes-Taylor integration [1]. This integration method applies a controlled amount of damping to high-frequency oscillations which aids convergence to steady-state deformation. The magnetic equations are solved using an H(curl)-conforming Galerkin method with implicit time integration [2]. The elastic equations and the magnetic equations are coupled using an operator-splitting approach. The software is based on an existing magnetohydrodynamics code [3], with the addition of the hyperelastic Mooney-Rivlin model for the stress-strain relationship. The computational mesh includes the film and a region of vacuum surrounding the film. In the film the mesh moves with the material (pure Lagrangian) but in the vacuum around the film the mesh is allowed to relax (ALE). This ALE relaxation prevents the mesh from becoming highly distorted for large film displacements.

A steel ring with a prescribed current is located above the film to create a magnetic field similar to a magnetic dipole. The distance between the mid-plane of the film and the mid-plane of the ring is $h$, see Fig. 2 for a schematic of the problem (definitions of undefined variables to follow in sections II and III). To minimize the size of the problem the axisymmetry of the system is used to mesh only a quarter of a revolution around the axis of symmetry and impose a symmetry boundary condition on the $x = 0$ and $y = 0$ planes. We also take advantage of the fact that the magnetic field produced above and below the center of the current carrying ring is symmetric, the $z = 2h$ plane. Thus we only mesh the region

below the center of the current carrying ring. See Fig. 3 and 4 for the FEM layout and material regions.

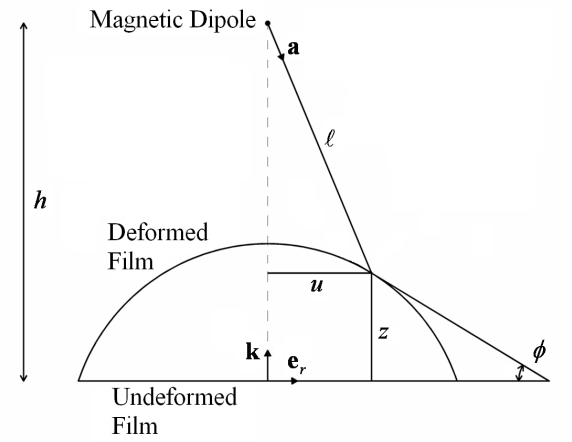


Fig. 2. Geometry of the membrane and the dipole source

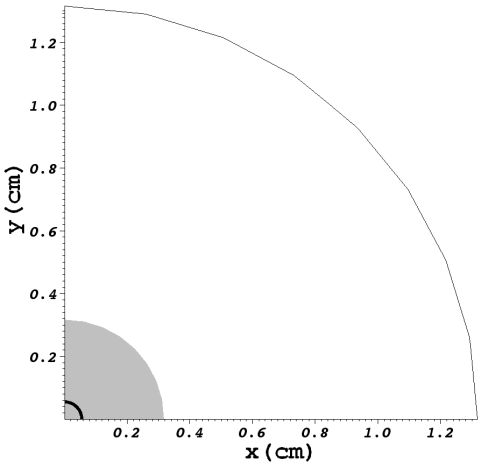


Fig. 3. Top view of FEM material regions (air is white, steel is black, film is gray)

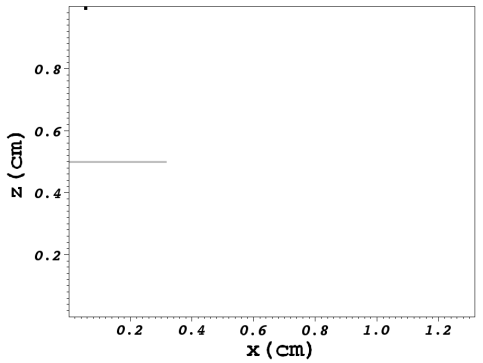


Fig. 4. Side view of FEM material regions (air is white, steel is black, film is gray)

The magnetic boundary conditions are as follows: on the ends of the current carrying ring at $y = 0$ the normal component of the current density is set to $J$ and on the other end of the wire at $x = 0$ the normal component of the current density is set to $-J$; on all other free surfaces the normal component of the current density is set to zero; on the top of the mesh (symmetry plane at $z = 2h$) the tangential component of the magnetic field is set to zero; on all other faces the tangential electric field is set to zero, thus insuring that the normal component of the magnetic field is zero

On all free surfaces that are not symmetry planes the displacement is constrained. The displacement on the edge of the film that is not on a symmetry plane is also constrained. The entire edge of the film is not constrained since this would impose zero slope as well as the desired zero displacement. To get a better comparison to the continuum model, only the nodes on the mid-plane are constrained. This constraint allows for rotation at the edge of the film while maintaining zero displacement of the mid-plane at the edge.

The elastic response of the film is modeled using the Mooney-Rivlin strain-energy function ($w$), in terms of the principal stretches [4]:

$$w(\lambda_1,\lambda_2,\lambda_3) = \tfrac{1}{2}G\begin{bmatrix}\delta\left(\lambda_1^2+\lambda_2^2+\lambda_3^2-3\right)+\\ (1-\delta)\left(\lambda_1^{-2}+\lambda_2^{-2}+\lambda_3^{-2}-3\right)\end{bmatrix} \quad (1)$$

where $G$ is the shear modulus; $\delta$ is a fixed material parameter and $\lambda_1$, $\lambda_2$ and $\lambda_3$ are the principal stretches.

Since the current carrying loop does not produce an exact magnetic dipole field, an equivalent dipole strength ($D_{eq}$) for comparison of the two methods needs to be calculated. The ALE finite element code is initially run in static mode (no motion) to determine the steady state magnetic field. An equivalent dipole strength is calculated for each element between $0 \le r \le r_0$ and $(h+\varepsilon/2) \le z \le 7h/5$, where $r_0$ is the radius of the film and $\varepsilon$ is the thickness. The equivalent dipole strength is calculated based on the z-component of the magnetic field ($h_{zALE}$), since it is larger than the radial component. The average of these values is used to calculate the equivalent dipole strength. The dipole magnetic field used in the continuum model is:

$$\mathbf{h} = h_z\mathbf{k} + h_r\mathbf{e}_r = D\frac{3(\mathbf{a}\cdot\mathbf{k})\mathbf{a}-\mathbf{k}}{\ell^3} \quad (2)$$

where $h_r$ and $h_z$ are the radial and axial components of the magnetic field, $D$ is the dipole strength, $\mathbf{a}$ is the unit vector from the dipole to a material point, $\mathbf{k}$ is the unit vector in the axial direction, $\ell$ is the distance from the dipole to a deformed material point ($\ell^2 = u^2 + (h-z)^2$) and $u(r)$ and $z(r)$ are the radial and axial coordinates of a material point in the deformed configuration. The equivalent dipole strength is determined by taking the dot product of equation 2 with $\mathbf{k}$ and setting $h_z$ equal to the axial component of the magnetic field produced in the finite element code($h_{zALE}$) resulting in:

$$h_{zALE} = D_{eq}\frac{2(z_c-h)^2 - r_c^2}{\ell^5} \quad (3)$$

and when solved for the equivalent dipole strength:

$$D_{eq} = \frac{\ell^5 h_{zALE}}{2(z_c-h)^2 - r_c^2} \quad (4)$$

where $z_c$ is the height of the center of the element above the mid-pane of the film; and $r_c$ is the radial position of the center of the element away from the axis of symmetry. It should be noted that the relationship between the equivalent dipole strength and the current density is linear. Thus once the equivalent dipole strength is calculated for one current density the equivalent dipole strength for any other current density can easily be calculated.

Once the equivalent magnetic field is determined the finite element code is used in the dynamic mode. In order to avoid an undesirable shock to the film, the magnitude of the current is slowly ramped up to the final value. The deformation as a function of the current magnitude is then recorded for comparison to the analytic model.

## III. Continuum Model

The analytical method is based on the membrane approximation, which will only be outlined here; see reference [4] for a complete derivation. The membrane approximation takes advantage of a small aspect ratio between the thickness and radius of the film, and an asymptotic expansion of the three-dimensional equations of static equilibrium about an aspect ratio of zero is taken. The leading order terms of this expansion form the membrane model. This approximation results in a model where rigidity with respect to bending is neglected. Refer to [4] for the derivation of the coupled first ordered system of differential equations presented here without proof:

$$\mu' = \left(r\hat{w}_{\mu\mu}\right)^{-1}\left[\begin{array}{l}\hat{w}_{\lambda}\cos\phi - \hat{w}_{\mu} - \hat{w}_{\lambda\mu}\left(\mu\cos\phi - u/r\right)\\ +r\dfrac{H}{\ell^6}\left\{\begin{array}{l}4(h-z)\dfrac{(h-z)^2}{\ell^2}\sin\phi\\ +\left[1+4\dfrac{(h-z)^2}{\ell^2}\right]u\cos\phi\end{array}\right\}\end{array}\right],$$

$$\lambda = u/r, \quad \mu = \sqrt{(u')^2+(z')^2}, \quad \cos\phi = u'/\mu, \quad \sin\phi = -z'/\mu, \tag{5}$$

$$\phi' = (r\hat{w}_{\mu})^{-1}\left[\begin{array}{l}-\hat{w}_{\lambda}\sin\phi +\\ r\dfrac{H}{\ell^6}\left\{\begin{array}{l}4(h-z)\dfrac{(h-z)^2}{\ell^2}\cos\phi\\ -\left[1+4\dfrac{(h-z)^2}{\ell^2}\right]u\sin\phi\end{array}\right\}\end{array}\right]$$

where $r \in [0, r_0]$ is the radius from the axis of symmetry of a material point in the reference configuration; $\lambda(r)$ and $\mu(r)$ are the azimuthal and radial principal stretches; $\phi(r)$ is an angle defined in Fig. 2; $\hat{w} = \varepsilon w$; $w$ is the conventional strain energy function dependent on the principal stretches; $H = 3D^2\mu_0\chi\varepsilon$; $\mu_0$ ( >0) is the free-space permeability; and $\chi$ is the magnetic susceptibility of the film. Refer to Fig 2 for a geometric representation. Note that the notation $()' = d()/dr$ and Greek or Latin subscripts are used to denote partial derivatives.

For our problem, making use of incompressibility and the relation between $w$ and $\hat{w}$ we arrive at the strain energy function:

$$\hat{w}(\lambda,\mu) = \frac{\varepsilon G}{2}\left[\begin{array}{l}\delta\left(\lambda^2+\mu^2+\lambda^{-2}\mu^{-2}-3\right)+\\ (1-\delta)\left(\lambda^{-2}+\mu^{-2}+\lambda^2\mu^2-3\right)\end{array}\right] \tag{6}$$

The above system (equation 5) is solved for the equilibrium of the deformed film using a shooting method--note that the dynamic stability of this solution is unknown.

## IV. Results

All results reported here are for a magnetoelastic film with the following properties and dimensions: radius of the film ($r_0$) of 0.317*cm*; dipole height ($h$) of 0.5*cm*; film shear modulus ($G$) of 0.25*MPa*; Mooney-Rivlin material property ($\delta$) of 0.9; film magnetic susceptibility ($\chi$) of 2.5; a variety of film thicknesses ($\varepsilon$) and dipole strengths ($D$).

When the magnetic field of the FEM model is compared to that of a dipole (equation 2), for elements used to calculate the equivalent dipole strength, the average error in the radial and axial direction is 3.3% and 1.7% respectively. This is quite good considering the different approximations used.

Fig. 5 shows the deformed position of the mid-plane of the film based on the membrane model at equilibrium, and Fig. 6 shows the deformed position of the film from the FEM, both at various dipole strengths. If the equivalent magnetic diapole strength of the FEM model is increased above 0.0059 $Am^2$ the FEM model becomes unstable (dynamic) and no static equilibrium is attained.

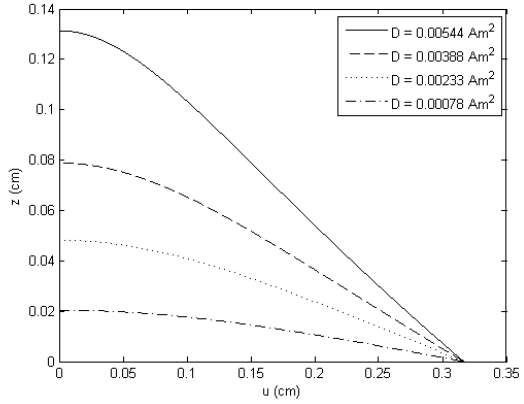


Fig. 5. Mid-plane displacement for membrane model

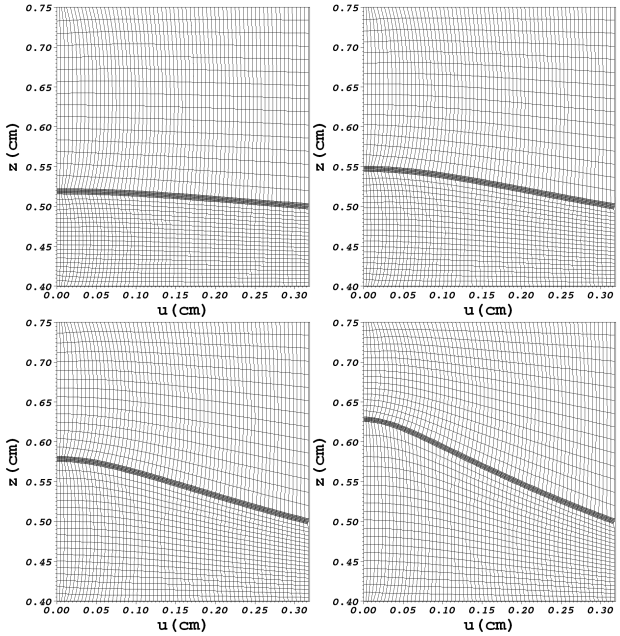


Fig. 6. FEM displacements for $\varepsilon$ = 70 $\mu m$ for $D$ = (0.00078, 0.00233, 0.00388 and 0.00544) $Am^2$

## V. Comparison and Conclusion

Two comparisons are made below. Fig. 7 has a comparison of the mid-plane deformation for a variety of dipole strengths. It is seen that the deformations for the two methods are very

similar, validating the FEM methods. Fig. 8 has a comparison of the mid-plane displacement at the center of the disk for a variety of dipole strengths. The two models agree well for the stable equilibria. We have also plotted unstable equilibria predicted by the membrane model ($z_0$>0.15); the dynamic FEM model does not find these solutions because the membrane snaps onto the dipole; see reference [5] for more detail on the membrane instability.

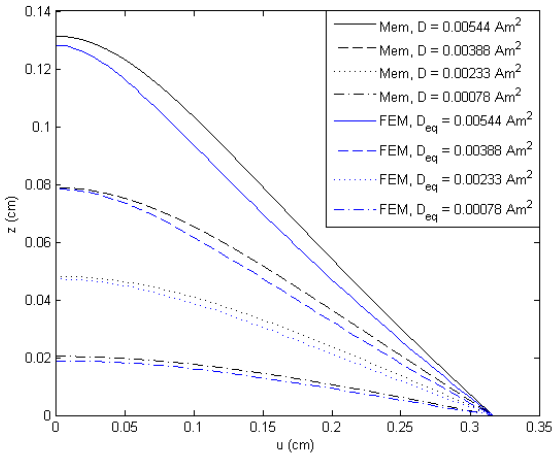


Fig. 7. Comparison of the mid-plane deformation for the continuum model (Mem) and FEM at $\varepsilon = 70\ \mu m$ for a range of dipole strengths *D*.

Comparisons of the mid-plane displacement at the center of the film were also made for varying film thickness for a variety of small dipole strengths, see Fig. 9. It is seen that as the thickness of the film in the FEM decreases it approaches the membrane model as expected.

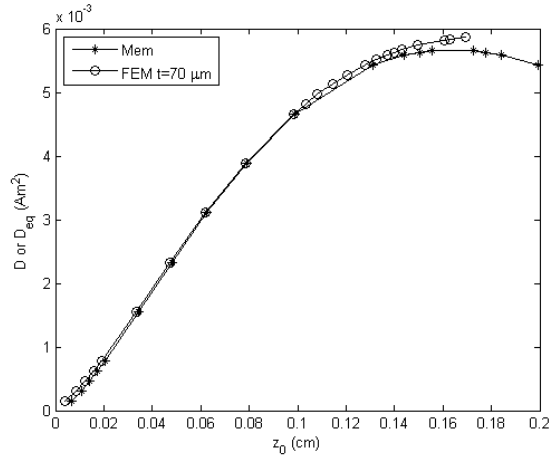


Fig. 8. Comparison of the z-displacement at the center of the film for the two methods at various dipole strengths *D*.

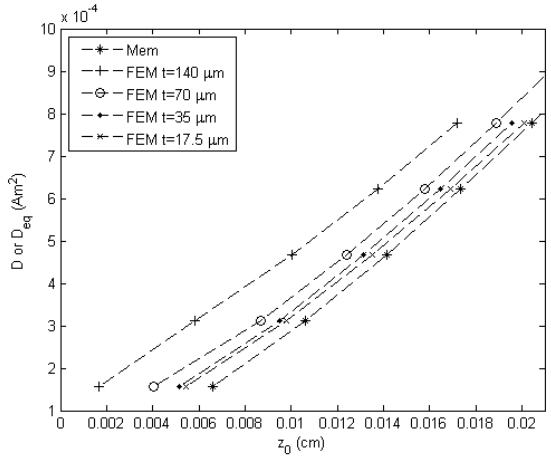


Fig.9. Comparison of the z-displacement at the center of the film for the two methods for small dipole strengths.

The good agreement of the results from the FEM and membrane models provides some validation of the FEM model. Based on this validation we have more confidence to apply the FEM model to obtain solutions to a broad array of problems including low-symmetry and dynamic magnetoelastic problems for which exact solutions are unattainable.

## ACKNOWLEDGMENT

This work was performed under the auspices of the U.S. Department of Energy by Lawrence Livermore National Laboratory under contract DE-AC52-07NA27344. LLNL-CONF-412042

## REFERENCES

[1] Hughes, T. J. R, *The Finite Element Method: Linear Static and Dynamic Finite Element Analysis*, Dover Publications, 1987.

[2] R. Rieben, D. White, "Verification of high-order mixed finite element solution of transient magnetic diffusion problems," *IEEE Trans. Magn.*, v. 42, n. 1, pp 25-39, 2006.

[3] R. Rieben, D. White, B. Wallin, J. Solberg, "An arbitrary Lagrangian-Eulerian discretization of MHD on 3D unstructured grids," J. Comp. Phys. 226, pp. 534-570, 2007.

[4] Barham M, Steigmann D J, McElfresh M and Rudd R E, "Finite deformation of a pressurized magnetoelastic membrane in a stationary dipole field" *Acta Mech.* vol. 191, pp. 1-19, 2007.

[5] Barham M, Steigmann D J, McElfresh M and Rudd R E, "Limit-point instability if a magnetoelastic membrane in a stationary magnetic field" *Smart Mater. Struct.* vol. 17, pp. 6-11 2008

Manuscript received March 6, 2009 Corresponding author: M. Barham (e-mail: barham2@llnl.gov;).